Emergency Power System Control Following A Saddle Node Bifurcation

Thomas J. Overbye
overbye@ece.uiuc.edu

Raymond P. Klump
ray@ece.uiuc.edu

Department of Electrical and Computer Engineering
University of Illinois at Urbana-Champaign
Urbana, IL 61801

Abstract

Restructuring in the electric power industry will result in system operation at higher levels of loading, increasing the potential for voltage instability due to a saddle node bifurcation. In this paper we present a computationally efficient method for emergency system control following such an event. The method only needs information typically available from a state estimator; it does not require the user to supply detailed models of system dynamics.

1. Introduction

The electric power industry in the United States is in the midst of a fundamental restructuring, with the previous structure of vertically integrated utilities providing electric power a regulated rates giving way to a more competitive marketplace with equal access to the transmission system for all wholesale buyers and sellers [1]. Such changes will undoubtedly also have profound effects on the nature of power system operations. While the specifics can be difficult to predict, we believe that increased competition we result in a much more heavily loaded transmission system with loading limits dictated more by voltage stability, rather than transient or thermal, considerations. One of the consequences of operating the system closer to its voltage stability boundary will be an a greatly increased potential for contingent situations in which system loadability limits are exceeded with the system subsequently experiencing a saddle node or Hopf bifurcation.

Over the last several years there has been a substantial amount of research done either to quantify the distance of a stable operating point from such a bifurcation or to determine the best way to mitigate a contingency which has pushed this desired operating point past the loadability boundary so that the power flow solutions no longer have a real solution. Many of the more recent contributions are described in [2] and [3]. However much of this research has been done from a "planning" perspective, in which a detailed knowledge of system dynamic parameters is assumed. With such knowledge it is possible to obtain either for a stable system a precise measure of distance to bifurcation, or for an unstable or unsolvable system a precise time simulation of the system response. But a difficulty with such an approach is that system behavior is often quite sensitive to the values of these dynamic parameters. For example in [4] and [5] the determination of system stability is shown to be quite sensitive to the assumed values of load parameters.

The accuracy of these assumed parameter values is probably best described as mixed. With the current vertically integrated utility structure planners usually have access to the values of the dynamic parameters of their own generators and often those of their neighboring competitors. While most of these assumed values are correct, testing is often needed to account for differences between assumed and actual system response. For loads parameter values, and even the models themselves, are at best difficult to determine. Limited testing of the dynamics of actual system loads has been helpful, but even a vertically integrated utility with a vested interest in accurate system modeling is quite reluctant to willing subject their customers to the substantial voltage deviations necessary to develop accurate models of load dynamics. Complicating model determination is the fact that system load is time dependent with, for example, the dynamics of an electric heating load quite different from that of air conditioning load. As the industry disaggregates into independent generation and distribution entities, determination of these dynamic parameters will become even more difficult. Enhanced customer choice of energy suppliers coupled with greater usage of dispersed energy storage devices, power electronic controllers, and real-time pricing will further exacerbate this situation.

However we believe these changes will actually serve to increase the controls available to the transmission system operator. In particular the loads themselves will become much more controllable as some customers opt for less reliability in return for lower prices. This could take the form of either direct load control through mechanisms such as interruptable contracts or indirect control through mechanisms such as real-time pricing. Direct communication and microprocessor control could permit such load controls to have response rates on the order of seconds.

The availability of such controls will permit system operation at high loading levels. However to achieve this level of operation it is important that control algorithms be developed to rapidly determine corrective control actions following potentially insecure contingencies. Yet these algorithms must not be dependent upon a detailed knowledge of system dynamic parameters since they would probably not be available in real-time. In this paper we propose such a method for the case in which the system (typically following a contingency) loses its equilibrium point via a saddle node bifurcation. For such a case if control action is not taken sufficiently quickly following the contingency which pushed the system into this unsolvable state, the system will never reach an acceptable equilibrium state. Rather, its state will vary as dictated by system dynamics, with the usual consequence of a voltage collapse. The algorithm we propose only requires knowledge of static system parameters (e.g., transmission line impedances) and near real-time knowledge of the system state (available from a state estimator).

2. Models and Motivation

Consider the power flow equations for an n+1 bus system with m PV buses, n-m PQ buses and a slack bus

$$\mathbf{S} = \mathbf{f}(\mathbf{x}) \quad (1)$$

where **S** is a vector of the actual real power load minus generation at all buses except the slack and the actual reactive power load at all PQ buses

$$\mathbf{S} = [P_1,\ldots,P_n,Q_{m+1},\ldots Q_n]^T \quad (2)$$

and **x** is the vector of bus angles at all buses (except the slack) and voltage magnitudes at the PQ buses

$$\mathbf{x} = [\theta_1, \theta_2, \ldots, \theta_n, V_{m+1}, V_{m+2}, \ldots, V_n]^T \quad (3)$$

and **f** is the function of the bus power balance constraints

$$\mathbf{f} = [f_{p,1}(\mathbf{x}), f_{p,2}(\mathbf{x}),\ldots,f_{p,n}(\mathbf{x}), f_{q,m+1}(\mathbf{x}), \ldots, f_{q,n}(\mathbf{x})]^T \quad (4)$$

with

$$f_{p,i} = -V_i \sum_{j=1}^{n} V_j \,[G_{ij}\cos(\theta_i - \theta_j) + B_{ij}\sin(\theta_i - \theta_j)] \quad (5a)$$

$$f_{q,i} = -V_i \sum_{j=1}^{n} V_j \,[G_{ij}\sin(\theta_i - \theta_j) - B_{ij}\sin(\theta_i - \theta_j)] \quad (5b)$$

and **G** + j**B** the network bus admittance matrix. Regardless of system dynamics, the power balance constraints are always satisfied. The algorithm developed in this paper assumes that all the parameters and variables in the preceding equations are known with sufficient accuracy in near real-time (usually from a state estimation program).

While the algorithm developed in this paper does not depend upon detailed knowledge of dynamic parameters, a dynamic model is needed to motivate and verify this method. Since the focus of the paper is on the longer term time frame in which operator intervention is possible, an assumption is made that initially following the instigating contingency the system is transiently stable with the pertinent dynamics those associated with the loads rather than the generators (other than generator excitation system reactive power limits).

System dynamics can be included by augmenting the static power flow equations to include dynamic load models. In keeping with the assumption that only load dynamics are pertinent, generators are represented using the standard power flow PV bus model (i.e., constant real power and voltage magnitude) provided their reactive power is with their limits, and by the PQ bus model if the reactive output attempts to exceed these limits. To represent dynamic load a number of different models have been proposed, with one popular model motivated by the fact that many loads are equipped with regulators (including down-stream LTC transformers) which, when modeled in aggregate, vary the load according to a generic first order model [6], [7], [8], [9], [10]:

$$T_{p,i}\,\dot{\lambda}_{p,i} = P_{s,i}(V_i) - P_i(V_i,\lambda_{p,i}) := \Delta P_i(\mathbf{x}) \quad (6a)$$

$$T_{q,i}\,\dot{\lambda}_{q,i} = Q_{s,i}(V_i) - Q_i(V_i,\lambda_{p,i}) := \Delta Q_i(\mathbf{x}) \quad (6b)$$

where

$T_{p,i}$, $T_{q,i}$ = positive time constants

$P_{s,i}(V_i)$, $Q_{s,i}(V_i)$ = desired (steady-state) load demand

$P_i(V_i,\lambda_{p,i})$, $Q_i(V_i,\lambda_{p,i})$ = actual (dynamic) load demand

$\lambda_{p,i}$, $\lambda_{q,i}$ = state variables associated with the load

Assume that the voltage dependence in the steady-state and dynamic load demand is modeled using the exponential model

$$P_{s,i}(V_i) = P_{o,i}V_i^a \quad (7a)$$

$$Q_{s,i}(V_i) = Q_{o,i}V_i^b \quad (7b)$$

$$P_i(V_i,\lambda_{p,i}) = \lambda_{p,i}V_i^{\alpha} \quad (7c)$$

$$Q_i(V_i,\lambda_{p,i}) = \lambda_{q,i}V_i^{\beta} \quad (7d)$$

Anytime a physical system is modeled the dynamic power balance equations must be satisfied. That is, when modeling a real system there must always be a set of voltages **x** that satisfies

$$\lambda_{p,i}V_i^{\alpha} = P_i(V_i,\lambda_{p,i}) = f_{p,i}(\mathbf{x}) \quad (8a)$$

$$\lambda_{q,i}V_i^{\beta} = Q_i(V_i,\lambda_{q,i}) = f_{q,i}(\mathbf{x}) \quad (8b)$$

In [11] it is shown that this condition is met provided all the coefficients α and β are greater than one. However there is no such requirement that the system be able to supply the desired load demand. Define the desired equilibrium point as

$$\mathbf{S}_s(\mathbf{x}) = [P_{s,1},\ldots,P_{s,n},Q_{s,m+1},\ldots Q_{s,n}]^T \quad (9)$$

Then for an unsolvable case

$$\mathbf{S}_s(\mathbf{x}) = f(\mathbf{x}) \quad (10)$$

does not have a real solution [12]. For such an unsolvable case (6) does not have an equilibrium point, with the subsequent system trajectory usually characterized by a sustained decline in voltage magnitudes. The time frame of this voltage decline is dependent upon the values of the time constants $T_{p,i}$ and $T_{q,i}$; values of several minutes are suggested in [7]. Therefore if control is not applied sufficiently quickly after the contingency the system will ultimately experience a voltage collapse.

To illustrate this problem, consider a three bus system with the pre-contingent operating point in Figure 1 (voltages and line impedances are per unit using a 100 MVA base). With the load model from (6), assume that the desired real power load has no voltage dependent (i.e., $a_1 = a_2 = 0$) while the dynamic real power load varies as the square of the voltage (i.e., $\alpha_1 = \alpha_2 = 2$) with the time constants $T_{p,1}$ and $T_{p,2}$ equal to 30 seconds each.

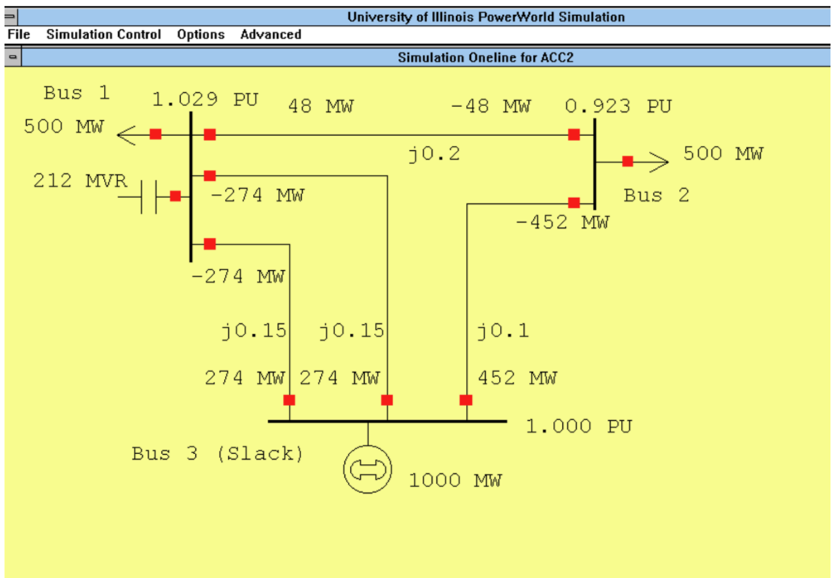

Figure 1: Three Bus Pre-contingent Case

With the outage of one of the lines from bus 1 to bus 3 the case would be unsolvable with (6) no longer having an equilibrium point Thus the power system can no longer supply the desired steady-state load demand of 500 MW at buses 1 and 2. However because of the dynamic load model, the dynamic power balance equations, (1) and (8), still have a solution, with the system state immediately after the contingency shown in Figure 2. The key point is that without a detailed knowledge of the load dynamics, the operator would not immediately know that anything was amiss (other than the somewhat reduced voltage at bus 2). The state estimator would provide the Figure 2 results which correspond to a valid and (statically) operable solution. An indication that something is wrong would only come over time as the voltages start to gradually decline, shown in Figure 3, driven by the load dynamics.

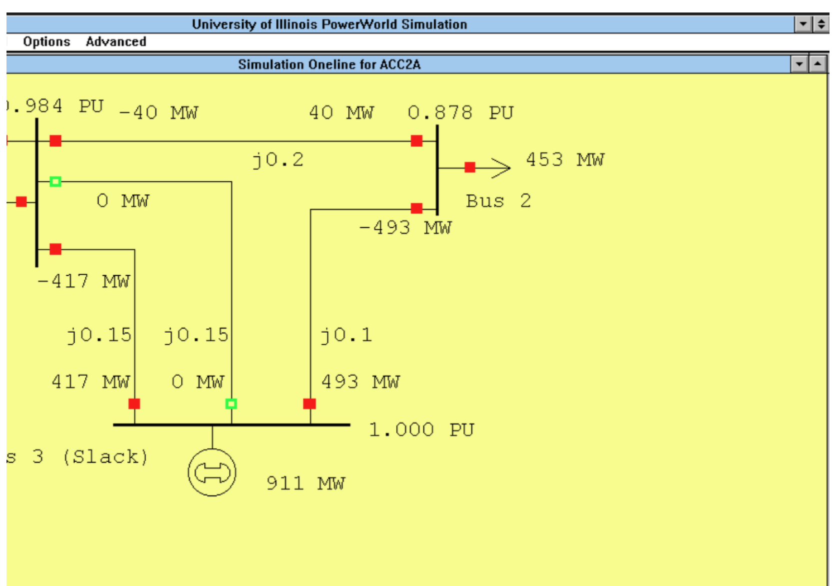

Figure 2: Three Bus Case Immediately after the Contingency

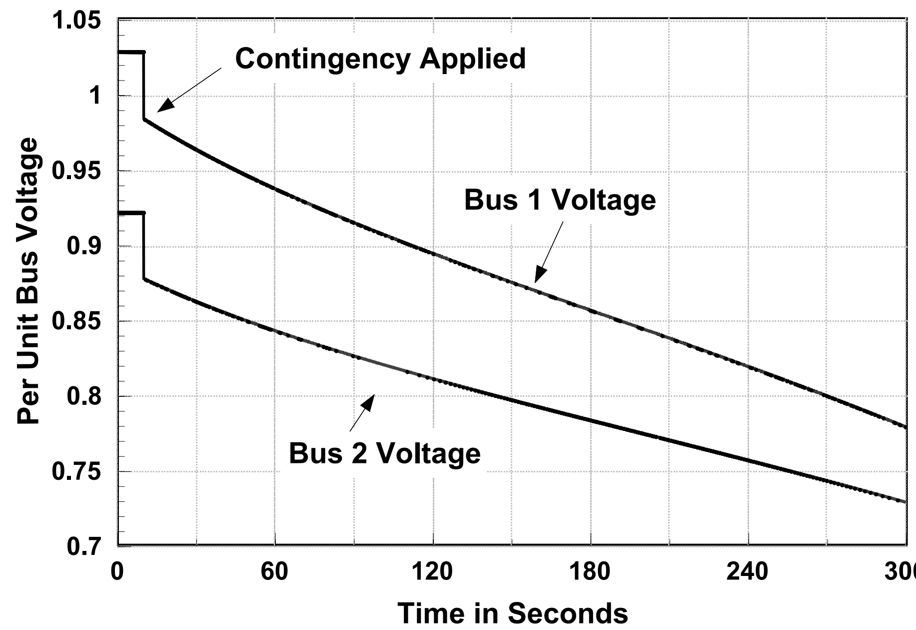

Figure 3: Three Bus Voltage Decline

The mechanics of this voltage decline can be explained with the aid of Figures 4 and 5. Regardless of the desired (steady-state) load, the network power balance equations constrain the system state to the hypersurface upon which these equations are satisfied. The dimension of this hypersurface is usually equal to the number of voltage states plus the number of power injections. The well-known PV curve simply shows a two-dimensional slice of this higher dimensional surface. Likewise the desired load defines a hyper-surface in the same space, with the system equilibrium points corresponding to the intersection points of these two hypersurfaces. Figure 4 shows the pre-contingent and post-contingent bus 1 PV curves along with the desired steady-state load. Note that the post-contingent PV curve no longer intersects the desired steady-state load. Therefore no post-contingent equilibrium point exists, with the system differential equations driving the state out to the maximum loadability boundary, and then downward along the bottom side of the hypersurface. Similarly, Figure 5 shows the projection this hypersurface into the P_1-P_2 space. The maximum loadability boundary is denoted by Σ with the desired equilibrium point outside this boundary in the unsolvable region.

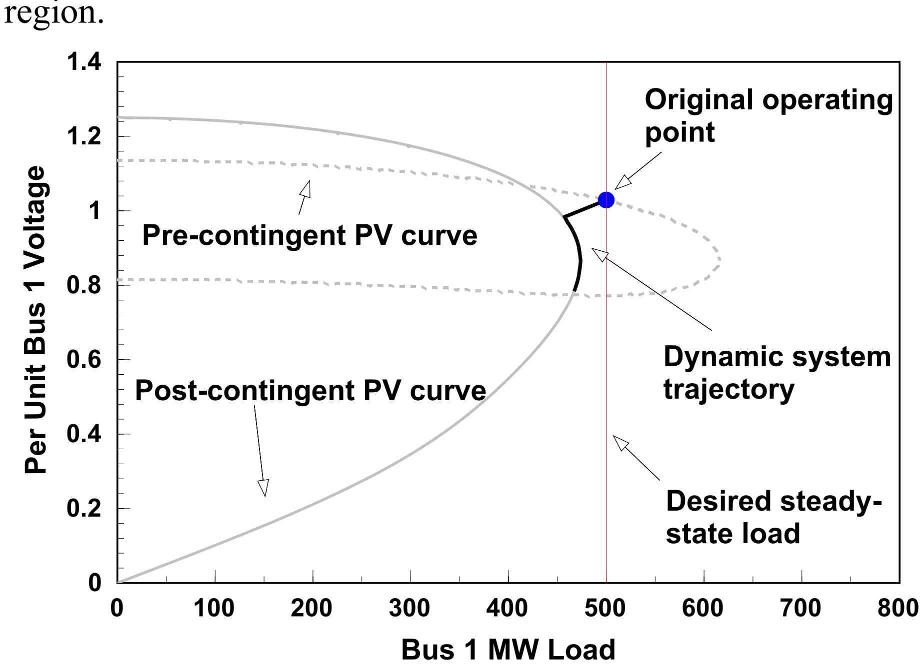

Figure 4: PV Bus Interpretation

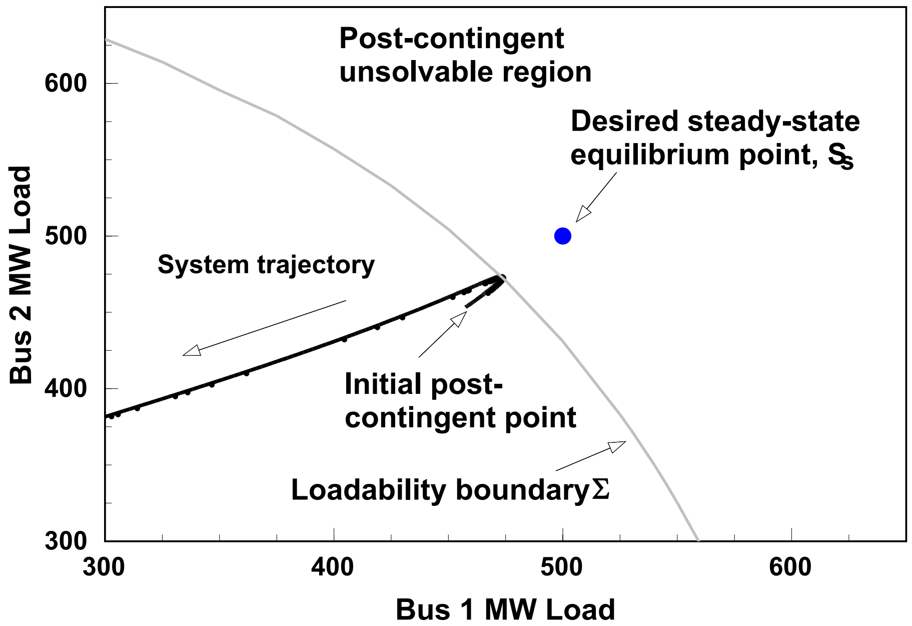

Figure 5: Load Parameter Space Interpretation

3. Determination of Effective Controls

The best algorithm to determine the set of controls necessary to restore such an unsolvable system to a secure operating point is very dependent upon assumptions about both the available information and the available time frame to solve the problem. For example if complete models for system dynamics are available along with a knowledge of the desired system equilibrium point, an iterative time domain simulation algorithm could be used in an off-line environment. A fast method simulation method, applicable to the time frame of this problem, is described in [13]. A more direct approach, but with restrictions on system dynamics, would be to use the energy based approach of [14]. While such approaches are certainly useful in a planning environment, we believe the difficulty in obtaining accurate dynamic load models will limit their applicability for on-line usage.

Assuming accurate dynamic models are not available but the user knows the desired system equilibrium, $\mathbf{S}_s$, then the method from [12] can be first used to quantify the unsolvability of the case. This is accomplished using a power flow based technique to determine the closest boundary point, defined as $\mathbf{S}_S^m$, to the desired equilibrium point. The Euclidean distance between these points, given by

$$D = \| \mathbf{S}_S^m - \mathbf{S}_s \| = \sqrt{[\mathbf{S}_S^m - \mathbf{S}_s]^T [\mathbf{S}_S^m - \mathbf{S}_s]} \qquad (11)$$

is then used to measure the unsolvability of $\mathbf{S}_s$. Then, using the result from [15] the sensitivities of D with respect to system controls, defined as $\mathbf{u}$, are given by

$$D_{\mathbf{u}} = -\mathbf{w}^m [\mathbf{f}(\mathbf{x}^m) - \mathbf{S}_s]_{\mathbf{u}} \qquad (12)$$

where $\mathbf{x}^m$ is the set of voltages corresponding to the closest boundary point, $[\mathbf{f}(\mathbf{x}^m) - \mathbf{S}_s]_{\mathbf{u}}$ is the Jacobian of the steady-state power balance equations with respect to the system controls $\mathbf{u}$, and $\mathbf{w}^m$ is the normalized left eigenvector associated with the zero eigenvalue of $\mathbf{J}(\mathbf{x}^m)$. The sign ambiguity of the eigenvector $\mathbf{w}^m$ (outward or inward from Σ) is resolved by choosing it to always be directed outward (i.e., sign of $\mathbf{w}^m$ is chosen so that $(\mathbf{S}_S^m - \mathbf{S}_s) \bullet \mathbf{w}^m > 0$). For the example from the previous section D = 0.263, with the sensitivity of D to changes in different load injections shown in Table 1.

Control (per unit)	ΔP_1	ΔQ_1	ΔP_2	ΔQ_2
Sensitivity $D_{\mathbf{u}_i}$	0.584	0.587	0.418	0.433

Table 1: Sensitivities of D to Control Changes

For this example the determination of $\mathbf{S}_s$ was straightforward, being equal to the pre-contingent system loading. However in many situations this point can be difficult to ascertain, particularly when the voltage instability is not directly preceded by a contingency. While the system may be placed in a vulnerable condition as a result of an earlier contingency, the actual voltage instability is driven by a gradual increase in the desired system loading, $P_{o,i}$ and $Q_{o,i}$. For example Figure 6 shows the voltages for the three bus case as the desired system loading is increased from 400 MW to 500 MW over a 20 minute time interval, while Figure 7 compares the desired to actual load over the same time period. Note that the state estimator would only provide the user with the actual system load; the desired load would not be known.

Without a knowledge of $\mathbf{S}_s$ it would be difficult to ascertain the voltage stability of the system from a single state estimator snapshot. But by observing the change in the voltages over time, the stability status of the system becomes much more apparent. However once the operator has determined that an insecure situation exists, there is still a need to determine the best controls to drive the system back towards a secure operating point. In the next section we present such a method, using only information provided by the state estimator.

4. Emergency System Control

Following the detection of a voltage instability the operator needs to quickly know the most effective control actions to avert voltage collapse. In this section we present an approach for solving this problem using only a knowledge of the current system state, $\mathbf{x}$, the time variation in the state, $\dot{\mathbf{x}}$, and the static network equations, $\mathbf{f}(\mathbf{x})$. Since the dynamic power balance

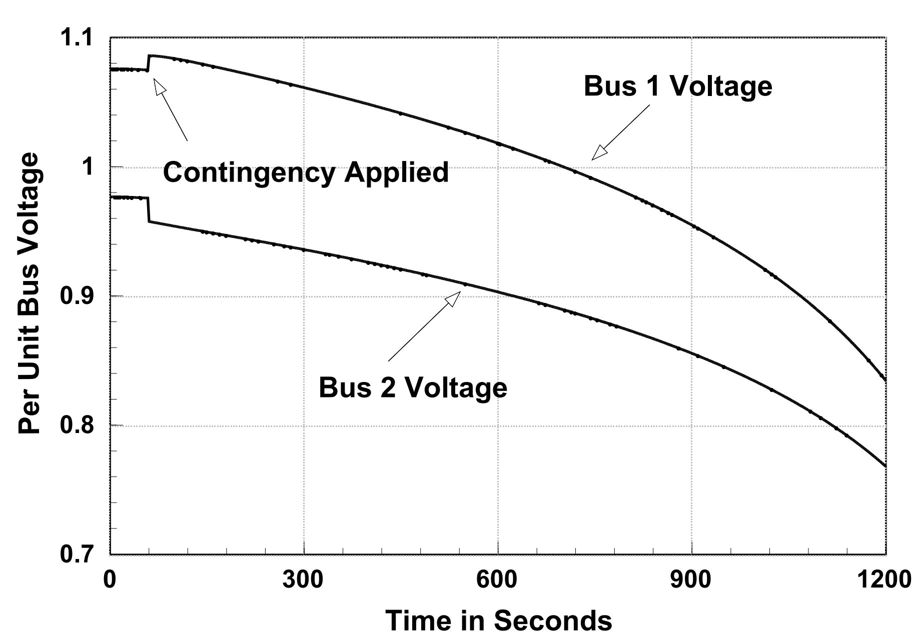

Figure 6: Three Bus Case with Gradual Load Variation

equations, (8), are always satisfied, we also know $P_i(V_i,\lambda_{p,i})$ and $Q_i(V_i,\lambda_{q,i})$.

From Figure 4 it is clear that during a system instability the system state may be either on the upper surface of the network constraint hypersurface, on the lower surface, or instantaneously, at the point of maximum loadability. When the state is at the maximum loadability point the Jacobian of (8), $\mathbf{J}(\mathbf{x})$, is singular, with the optimal control direction given by the left eigenvector associated with the zero eigenvalue of $\mathbf{J}(\mathbf{x})$ [16], [15], [13]. For all other situations whether the state is on the upper or lower surface can be determined by examining the signs of the eigenvalues of $\mathbf{J}(\mathbf{x})$ (or of $-\mathbf{J}(\mathbf{x})$). If all the eigenvalues are positive, then the state is on the upper surface, while if one is negative then the state is on the lower surface. Since a matrix determinant is equal to the product of its eigenvalues, a quick way to determine whether the state is on the upper or lower surface is to examine the determinant of $\mathbf{J}(\mathbf{x})$ (easily calculated by taking the product of the diagonals of the factored Jacobian). If the determinant is positive the state is on the upper surface, otherwise the state is on the lower surface.

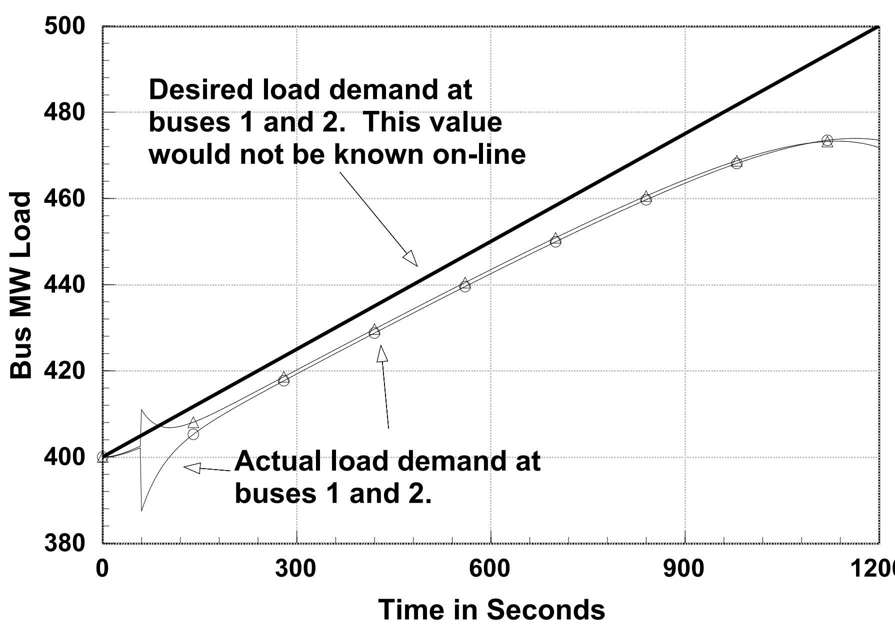

Figure 7: Three Bus Case Load Variation

To develop the algorithm, assume that the state $\mathbf{x}$ is an equilibrium point of the static power balance equations. Then, using a static load model there will be at least one close by alternative power flow solutions. If $\mathbf{x}$ is on the upper surface then this alternative point will be a type-one low voltage solution, while if $\mathbf{x}$ is on the lower surface this point will be the high-voltage solution of the power flow equations. Define the high-voltage solution as $\mathbf{x}^H$ and the low voltage solution as $\mathbf{x}^L$. The energy method [17] then provides a measure of the distance between these two points. Usually this energy measure is defined as the vector integration of the lossless power mismatch equations from $\mathbf{x}^H = \mathbf{x}$ to $\mathbf{x}^L$. However in this paper we introduce a slight variation for situations during which the system state is on the lower surface, that is, when $\mathbf{x} = \mathbf{x}^L$. In this case the integration is from $\mathbf{x}$ to $\mathbf{x}^H$ resulting in a negative energy value. For example Figure 8 shows the variation in the energy measure for the example described in Section 2, with a positive energy gradually decreasing to zero as the post-contingent trajectory reaches the maximum loadability boundary Σ and then going negative, indicating operation on the lower portion of the network constraint hypersurface.

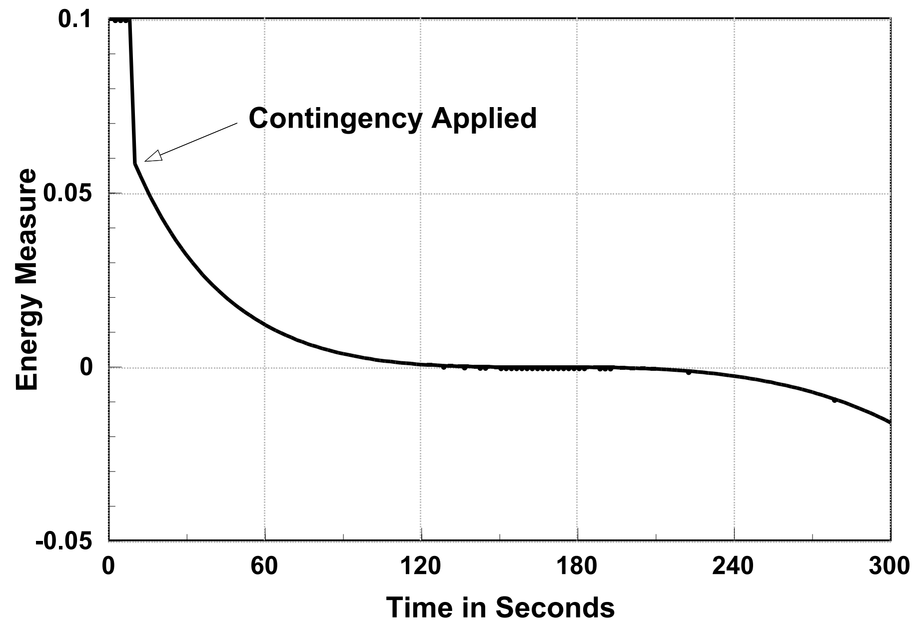

Figure 8: Energy Measure Variation for Section 2 Scenario

The energy measure itself provides a smoothly varying indicator of system instability. More importantly, however, [18] describes a computationally efficient method for calculating the sensitivity of the energy measure to various controls. The goal of emergency system control is to select the most effective controls to increase this margin. Since the energy measure is inherently a function of both the high and low voltage states, it must be emphasized that these sensitivities are not simply linearizations about the current operating point. Let

$\mathbf{u}$ = Potential control variables, including generator real power output, set point voltages, MW transactions, and MW/Mvar load injections.

$\vartheta(\mathbf{u}, \mathbf{x}^H, \mathbf{x}^L)$ = Energy measure, showing explicit and implicit dependence on the control variables.

Since the energy function depends upon the control variables both explicitly and implicitly, the first order sensitivites of the energy measure with respect to changes in the control variables can be calculated as

$$\frac{d\vartheta}{d\mathbf{u}} = \frac{\partial\vartheta}{\partial\mathbf{u}} + \frac{\partial\vartheta}{\partial\,\mathbf{x}^L}\frac{\partial\mathbf{x}^L}{\partial\mathbf{u}} - \frac{\partial\vartheta}{\partial\,\mathbf{x}^H}\frac{\partial\mathbf{x}^H}{\partial\mathbf{u}} \qquad (13)$$

Computationally the cost to calculate each control sensitivity is on the order of a forward and backward substitiution of the power flow equations, with further details provide in [18]. As an example, Figure 9 shows the normalized control sensitivities for changes in the real and reactive load at buses 1 and 2 for the Section 2 example. Note that the sensitivites remain fairly constant, and are nearly identical to the left eigenvector values shown in Table 1. The advantage of the energy approach is that the sensitivites can be calculated at any loading level; the user does not have to determine the point at which the trajectory reaches Σ. For this case the most sensitive control would be reducing real power at bus 1. Of course which control(s) to use depends upon other factors as well, including cost and availability. The advantage of knowing the normalized sensitivities is that it allows the operator to immediately begin intervention with the most effective controls. The need to begin control intervention as quickly as possible is particularly important in such situations in which the system has lost its equilibrium point; delay could be result in a large system collapse.

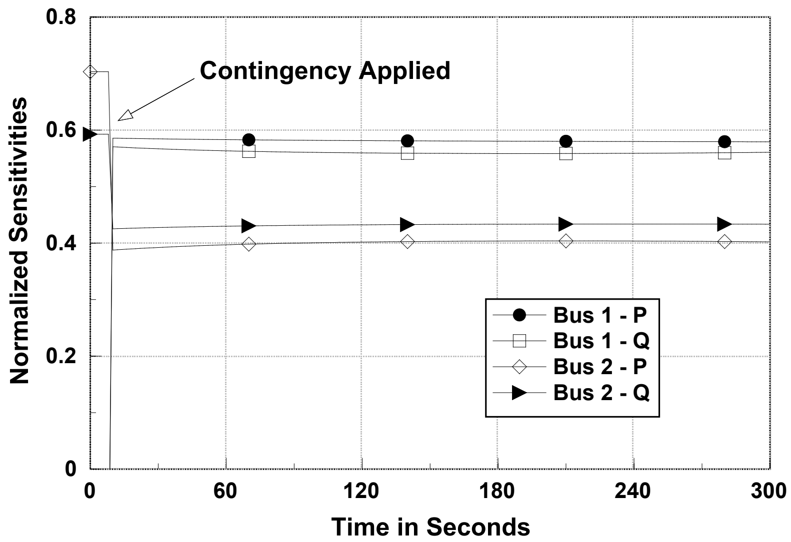

Figure 9: Normalized Control Sensitivities

5. Application to Larger Systems and Summary

This paper has introduced the idea of using energy techniques for emergency system control following a saddle node bifurcation. Once the operator has determined an emergency situation exists, the method determines the most sensitive controls for restoring the case to a solvable point. Following the determination of the current system state, the energy measure itself can be calculated with only one additional power flow solution. For the three bus case studied in this paper determination of this alternative power flow solution was straightforward (since there were only two solutions).

For larger systems, in which a number of altemative solutions may exist, we plan on using the method of [19] to search for the pertinent alternative solution, with the caveat that the search direction is given by the average time variation in the system state, X. This idea is motivated by recognizing that following a saddle node bifurcation the initial direction of the system state is along the right eigenvector associated with the zero eigenvalue of the polar form of the system Jacobian at the bifurcation point [20], and that at the midpoint between any two power flow solutions the Jacobian is singular with the right eigenvector associated with the zero eigenvalue pointing in the direction of the line segment joining these two solutions [19]. Future research will be directed towards testing this method on larger systems.

6. Acknowledgments

The authors would like to acknowledge the support of NSF through its grant NSF ECS-9209570 and the Power Affiliates program of the University of Illinois at Urbana-Champaign.

7. References

[1] Federal Energy Regulatory Commission of the United States of America, "Promoting wholesale competition through open access non-discriminatory services by public utilities," Docket No. RM95-8-00, March 1995.

[2] *Suggested Techniques for Voltage Stability Analysis*, IEEE 93TH0620-5PWR, 1993.

[3] *Proceedings Bulk Power System Voltage Phenomena III - Voltage Stability and Control*, Davos, Switzerland, Aug. 1994.

[4] C. Rajagopalan, B. Lesieutre, P.W. Sauer and M.A. Pai, "Dynamic aspects of voltage/power characteristics," *IEEE Trans. on Power Sys.*, vol. 7, pp. 990-1000, August 1992.

[5] T.J. Overbye, "Effects of load modelling on analysis of power system voltage stability," *Electrical Power & Energy Systems*, vol. 16, number 5, pp. 329-338, 1994.

[6] W. Xu and Y. Mansour, "Voltage stability analysis using generic dynamic load models," *IEEE Trans. on Power Sys.*, vol. 8, pp. 479-493, Feb. 1994.

[7] K.-M. Graf, "Dynamic simulation of voltage collapse processes in EHV power systems," *Proc.: Bulk Power System Voltage Phenomena-Voltage Stability and Security*, EPRI EL-6183, pp. 6.45-54, Jan. 1989.

[8] M.K. Pal, "Voltage stability conditions considering load characteristics," *IEEE Trans. on Power Sys.*, vol. 7, pp. 243-249, February 1992.

[9] C.W. Taylor, "Voltage stability part I: introduction, definitions, time frames/scenarios, and incidents, " *Survey of the Voltage Collapse Phenomenon*, NERC, pp. 51-65, August 1991.

[10] D. Karlsson and D.J. Hill, "Modelling and identification of nonlinear dynamic loads in power systems," *IEEE Trans. on Power Sys.*, vol. 9, pp. 157-166, February 1994.

[11] B.C. Lesieutre, P.W. Sauer and M.A. Pai, "Sufficient conditions for static load models for network solvability," *Proc. 24th North American Power Symposium*, pp. 262-271, Reno, NV, October 1992.

[12] T.J. Overbye, "A power flow measure for unsolvable cases," *IEEE Trans. on Power Sys.*, vol. 9, pp. 1359-1365, August 1994.

[13] T. Van Cutsem, Y. Jacquemart, J.-N. Marquet, and P. Pruvot, "Extensions and applications of mid-term voltage stability analysis method," *Proceedings Bulk Power System Voltage Phenomena III - Voltage Stability and Control*, pp. 251-262, Davos, Switzerland, Aug. 1994.

[14] T.J. Overbye, "Computation of a practical method to restore power flow solvability," *IEEE Trans. on Power Sys.*, vol. 10, pp. 280-287, February 1995.

[15] I. Dobson and L. Lu, "Computing an optimum direction in control space to avoid saddle node biufrcation and voltage collapse in electric power systems," *IEEE Trans. on Automatic Control*, vol. 37, pp. 1616-1620, October 1992.

[16] I. Dobson, "Observations on the geometry of saddle node bifurcation and voltage collapse in electrical power systems," *IEEE Trans. on Circuits and Sys.,* vol. 39, pp. 240-243, March 1992.

[17] C.L. DeMarco and T.J. Overbye, "An energy based security measure for assessing vulnerability to voltage collapse," *IEEE Trans. on Power Sys.,* vol. 5, pp. 582-591, May 1990.

[18] T.J. Overbye and C.L. DeMarco, "Voltage security enhancement using energy based sensitivities," *IEEE Trans. on Power Sys.*, vol. 6, pp. 1196-1202, August 1991.